Electron-impact detachment of weakly bound negative ions: Threshold and scaling laws

F. Robicheaux
Department of Physics, 206 Allison Laboratory, Auburn University, Alabama 36849-5311
and FOM Institute for Atomic and Molecular Physics, Kruislaan 407, 1098 SJ Amsterdam, the Netherlands
(Received 3 March 1999)

The details of a recent theoretical formulation of electron-impact detachment of weakly bound negative ions are presented. The formalism is applied at low energies to find the behavior of the cross section near threshold. Also, the applicability of a recently proposed scaling law is discussed. The formulation uses different coordinate systems for the initial and final states. The initial state is a simple product of wave functions of each electron, while the final state is a simple product of wave functions in center-of-mass coordinates.
[S1050-2947(99)08908-8]

PACS number(s): 34.80.Kw, 34.10.+x

I. INTRODUCTION

There have been several recent experiments measuring the electron-impact detachment cross section of atomic and molecular negative ions [1–8]. There have also been several calculations [9–15] that investigated this process. It is difficult to accurately calculate the detachment cross section because there are two free electrons in the final state and the theoretical studies all struggled with the large amount of correlation between the two free electrons. A wide variety of theoretical methods has been used to describe this process when the energy of the incident electron is several times the threshold energy. These methods have included an *R*-matrix pseudostate technique, distorted-wave Born approximations, a classical calculation of the threshold law, and semiclassical time-dependent methods.

The method used in Ref. [14] was based on a distorted-wave Born approximation, but is expected to be accurate at all energies, including the threshold region. The key insight into Ref. [14] was that, to a large extent, the final-state correlation is an illusion resulting from the use of the wrong coordinate system; how correlated a system appears depends on the coordinate system that is chosen to describe it. In the center-of-mass coordinate system for the two electrons, there is almost *no* correlation because the interelectron repulsion cannot cause interaction between the motion of the electrons' center-of-mass and interelectron degrees of freedom; the only way to exchange energy between the electrons' center-of-mass motion and the interelectron motion is for one of the electrons to scatter from the atom, which is not likely after the weakly bound electron has been detached. Thus, the final state distorted wave is expected to be a very good approximation to the exact wave function. The corresponding *T*-matrix elements and cross section calculated with this final state are expected to be correspondingly accurate.

The method can be described as a lowest-order distorted wave and Coulomb Born approximation. The initial state is given as an uncorrelated two-electron wave function where one electron is weakly bound to the atom and the wave function for the incoming electron is a distorted continuum wave that is asymptotically the solution for a repulsive Coulomb potential. The final state wave function is given as an uncorrelated wave function in center-of-mass coordinates. The wave function is taken to be the product of a plane wave for the center of mass and undistorted continuum waves for a repulsive Coulomb potential in the interelectron coordinate, $\mathbf{r}_2-\mathbf{r}_1$. This method differs from the usual implementation of distorted-wave theory because the final state is usually taken to be uncorrelated continuum waves of the individual electron's coordinates, $\mathbf{r}_1$ and $\mathbf{r}_2$. This difference is crucial because there is much less final-state correlation in the center-of-mass coordinates. Thus, the apparently crude method described in this paper is accurate because the double continuum final state in center-of-mass coordinates approximates the exact double continuum wave function very well.

The first purpose of this paper is to describe the practical implementation of this method in detail; there are several steps that can be made either less or more efficient than expected depending on the methods used. The second purpose is to use the method to calculate the total cross section and cross-section differential in the center-of-mass energy in the region near threshold. The results are compared to the different threshold laws from Refs. [15,16]. The present results indicate that it will be extremely difficult to measure the threshold law in the region where the formulation in Ref. [16] applies; the extended threshold law given in this paper gives an energy dependence that can be tested in the near future. The threshold law presented here confirms the origin of the dominant energy dependence discussed in Ref. [15]. Although the threshold law from Ref. [15] and this work are very similar, it should be possible to experimentally distinguish between them. The third purpose is to use the method to calculate the total detachment cross section for several binding energies of a negative ion and assess the applicability of a scaling rule for the cross section. Atomic units are used unless explicitly stated otherwise.

II. IMPORTANT THEORETICAL CONSIDERATIONS

In the electron-impact detachment of weakly bound negative ions, the main effects arise from the interaction between the incident electron and the extra electron on the atom. For the purposes of this paper, weakly bound means that the extra electron only has a small probability to be in the region of the atomic electrons. The probability of finding the excess

electron outside of the atom should be greater than ~90%. The reason for this restriction is that after the bound electron is detached from the atom there should be very little probability for one of the two continuum electrons to scatter from the atom. Since the incoming electron causes the detachment at large distances, it has a very small probability for scattering from the atom. However, the electron that was originally bound to the atom is relatively likely to scatter from the atom if it is tightly bound. Fortunately, the bound electron tends to gain angular momentum when it gains energy from the incoming electron and thus it cannot penetrate into the region of the atomic electrons *if* it originally has a large probability for being outside of the atom.

The restriction to being weakly bound removes almost all of the dependence on properties of the neutral atom. The cross section only depends on the angular momentum and binding energy of the weakly bound electron and on the asymptotic form of its wave function. The formalism described below is a two-electron method.

The basic approximation and insight into the dynamics may be obtained from a two-electron Hamiltonian in which each of the electrons interact with an infinitely heavy atom through a short-range potential $U(r)$. In atomic units, the Hamiltonian in the $\mathbf{r}_1,\mathbf{r}_2$ coordinate system is

$$H=-\tfrac{1}{2}\nabla_1^2-\tfrac{1}{2}\nabla_2^2+U(r_1)+U(r_2)+1/|\mathbf{r}_2-\mathbf{r}_1|. \qquad (1)$$

This clearly shows the difficulty in using this coordinate system to describe the final state since the $1/|\mathbf{r}_2-\mathbf{r}_1|$ potential causes correlation between the two electrons out to enormous distances; by correlation, I mean that there can be an exchange of energy and angular momentum between the $\mathbf{r}_1$ and $\mathbf{r}_2$ degrees of freedom. The Hamiltonian is useful in this form for understanding the behavior of the electrons in the initial state. One of the electron's wave function is an eigenstate of the one-electron Hamiltonian $-(1/2)\nabla^2+U(r)$ and the other electron's wave function is a continuum eigenstate of the screened repulsive Coulomb potential $-(1/2)\nabla^2+\tilde{U}(r)$. Thus the wave function for the initial state is a product of two one-electron functions to a good approximation.

The very strong final-state correlation is an artifact of describing the dynamics in the $\mathbf{r}_1,\mathbf{r}_2$ coordinate system. If we use the coordinate system $\mathbf{r}_\pm=(\mathbf{r}_2\pm\mathbf{r}_1)/\sqrt{2}$, then the Hamiltonian becomes

$$H=-\tfrac{1}{2}\nabla_+^2-\tfrac{1}{2}\nabla_-^2+1/(\sqrt{2}r_-)+U(|\mathbf{r}_++\mathbf{r}_-|/\sqrt{2})+U(|\mathbf{r}_+-\mathbf{r}_-|/\sqrt{2}). \qquad (2)$$

This Hamiltonian suggests that the final state is a product of the eigenstates of the $-(1/2)\nabla_+^2$ operator and the $(-1/2)\nabla_-^2+1/(\sqrt{2}r_-)$ operator. Now the correlation in the dynamics arises from the short-range potentials U. In the final state, these potentials are effectively zero since both r_1 and r_2 are large. However, this coordinate system gives a very poor description of the initial state because one of the electrons is near the atom. Thus, in the initial state, there is a very strong correlation between the motion in the $\mathbf{r}_-$ direction and the $\mathbf{r}_+$ direction.

Fortunately, there is no rule that forces the use of the same coordinate system for both the initial and final state; choosing the same coordinate system is simply a matter of convenience. The main insight in Ref. [14] is that it is practical to perform calculations with initial and final states in different coordinate systems. This increases the accuracy of a first-order distorted-wave Born approximation to the point where going to higher order is not necessary.

A. Basic formulation

The T-matrix element at energy E for scattering from channel i to j is

$$T_{ij}=\pi\int dV[(H_0-H)\psi_i^{(0)}]^*\psi_j^{(f)}, \qquad (3)$$

where both the initial and final states are energy normalized. This expression is exact if $\psi_j^{(f)}$ is the exact solution of $(E-H)\psi_j^{(f)}=0$ with the correct asymptotic boundary conditions. The relative size of the error in the T-matrix element is proportional to the size of the error in $\psi_j^{(f)}$. By using final states that accurately represent the double continuum final state, we greatly reduce the error in the T-matrix. If the final state is exact, the T-matrix does not depend on H_0 as long as the exact bound states are produced and the asymptotic form of the potential for the continuum electron is correct. This property gives a method for estimating the error in the calculation; the size of the variation of the cross section with different choices of H_0 is zero for exact $\psi_j^{(f)}$ and increases as the error in the final state increases.

The initial wave function is

$$\psi_i^{(0)}=\frac{1}{\sqrt{2}}\{R_{\ell_b}(r_1)F_{\ell_i}(r_2)[Y_{\ell_b}(\hat{r}_1)Y_{\ell_i}(\hat{r}_2)]_M^L \pm R_{\ell_b}(r_2)F_{\ell_i}(r_1)[Y_{\ell_b}(\hat{r}_2)Y_{\ell_i}(\hat{r}_1)]_M^L\}, \qquad (4)$$

where $R_{\ell_b}(r)Y_{\ell_b}(\hat{r})$ is the wave function for the weakly bound electron, $F_{\ell_i}(r)Y_{\ell_i}(\hat{r})$ is the wave function for the incident electron, and the two electrons are coupled to total angular momentum, L, with the z component being M (the notation $[YY]_M^L$ is meant to indicate that the two angular momenta are coupled using Clebsch-Gordon coefficients). The incident electron's wave function is the solution of a one-particle Hamiltonian with a potential $\tilde{U}(r)$ that has the form $1/r$ as $r\to\infty$; the proper choice for $\tilde{U}(r)$ for smaller r is discussed below. The incident continuum wave is normalized per unit energy. The $+$ $(-)$ in Eq. (4) is for the singlet (triplet) wave function.

The bound orbital is the space normalized solution of

$$\left[-\frac{1}{2r}\frac{\partial^2}{\partial r^2}r+\frac{\ell_b(\ell_b+1)}{2r^2}+U(r)\right]R_{\ell_b}(r)=E_bR_{\ell_b}(r), \qquad (5)$$

where ℓ_b is the angular momentum of the bound electron and E_b is its energy with respect to the detachment threshold. The potential $U(r)$ was chosen in a manner similar to that in Ref. [17]. The basic idea is that the binding energy and the asymptotic normalization of the $R_{\ell_b}(r)$ should match that of a more exact many-electron wave function [18,19].

The prescription for obtaining the short-range potential was not involved. The multielectron wave function was converted to a radial density by integrating over all of the electronic coordinates except for one radius. Outside the core region the density has the form

$$\rho(r)\rightarrow N_b^2\frac{\kappa_b}{r^2}e^{-2\kappa_b r}\quad\text{as}\quad r\rightarrow\infty, \tag{6}$$

where $\kappa_b=\sqrt{-2E_b}$ and N_b is a normalization constant that depends on the fraction of the weakly bound electronic wave function that is in the region near the electrons of the atom. The potential $U(r)$ was chosen so that the space normalized orbital $R_{\ell_b}(r)$ has the form

$$R_{\ell_b}(r)\rightarrow\sqrt{\kappa_b}\,\frac{N_b}{r}e^{-\kappa_b r}\quad\text{as}\quad r\rightarrow\infty \tag{7}$$

with the same N_b and κ_b as for the exact many-electron wave function. The only other restriction is that the range of $U(r)$ be roughly the size of the atom.

The incident continuum wave is the solution of

$$\left[-\frac{1}{2r}\frac{\partial^2}{\partial r^2}r+\frac{\ell_i(\ell_i+1)}{2r^2}+\tilde{U}(r)\right]F_{\ell_i}(r)=E_iF_{\ell_i}(r), \tag{8}$$

where $E_i=E-E_b$ is the incident energy. The radial function is normalized per unit energy so that at asymptotically large distances, it has the form

$$F_{\ell_i}(r)\rightarrow\frac{1}{r}\sqrt{\frac{2}{\pi k}}\sin\left[kr-\frac{1}{k}\log(kr)+\delta\right]\quad\text{as}\quad r\rightarrow\infty, \tag{9}$$

where $k=\sqrt{2E_i}$ is the wave number of the incident electron and δ is an energy dependent phase shift. The distorted-wave potential for the incident electron has been chosen to be

$$\tilde{U}(r)=[1-(1+\kappa_b r)e^{-2\kappa_b r}]/r, \tag{10}$$

which has the correct asymptotic form as $r\rightarrow\infty$ and mimics the screening from the weakly bound electron. If the final state were exact, then the results would be independent of $\tilde{U}(r)$ as long as $\tilde{U}(r)\rightarrow 1/r$ as $r\rightarrow\infty$. The results of the calculations were not very sensitive to the precise form of $\tilde{U}$ (10–15% changes were observed if the distorted-wave potential was set to $1/r$ for all r); the screened potential was chosen because it seems the results were slightly more accurate.

The final-state wave function is

$$\psi_f=\sqrt{\frac{2k_+}{\pi}}j_{\ell_+}(k_+r_+)f_{\ell_-}(r_-)[Y_{\ell_+}(\hat{r}_+)Y_{\ell_-}(\hat{r}_-)]^L_M, \tag{11}$$

where $E_+=k_+^2/2$, j_ℓ is the spherical Bessel function and $f_\ell(r)Y_\ell(\hat{r})$ is the solution of the Schrödinger equation for a repulsive Coulomb potential with charge $1/\sqrt{2}$. The f_{ℓ_-} and $\sqrt{2k_+/\pi}j_{\ell_+}$ are normalized per unit energy. The triplet wave function has ℓ_- equal to an odd integer while ℓ_- is an even integer for the singlet wave function. The energies for the initial state are the energy of the weakly bound electron, E_b, and the energy of the incident electron, E_i. The energies for the final state are the energy in the $+$ degrees of freedom, E_+, and the energy in the $-$ degrees of freedom, E_-. Conservation of energy means $E=E_b+E_i=E_++E_-$, where $0\leqslant E_+\leqslant E$.

The T-matrix elements are the important parameters for calculating the cross section. The initial and final states have the same symmetry for the operation $\mathbf{r}_1\leftrightarrow\mathbf{r}_2$ and both H and H_0 are symmetric with respect to this operation. This means that both terms in $\psi^{(0)}$ contribute equally to the T-matrix element. The T-matrix element will now be indexed with all relavent parameters to give an explicit expression:

$$\begin{aligned}T^L_{\ell_b\ell_i,\ell_-\ell_+}=\sqrt{4\pi k_+}\int dV_1dV_2\left[\tilde{U}(r_2)-U(r_2)-\frac{1}{r_{12}}\right]\\ \times j_{\ell_+}(k_+r_+)f_{\ell_-}(r_-)[Y_{\ell_+}(\hat{r}_+)Y_{\ell_-}(\hat{r}_-)]^L_M\\ \times\{R_{\ell_b}(r_1)F_{\ell_i}(r_2)[Y_{\ell_b}(\hat{r}_1)Y_{\ell_i}(\hat{r}_2)]^L_M\}^*.\end{aligned} \tag{12}$$

This is a six-dimensional integration that can be reduced to a five-dimensional integration because $\phi_1+\phi_2=\phi_++\phi_-$.

For a fixed E_+, the cross-section [20] differential in E_+ is

$$\frac{d\sigma}{dE_+}=\frac{2\pi}{E_i}\sum_{\ell_i\ell_+\ell_-LS}\frac{(2L+1)(2S+1)}{(2\ell_b+1)4}|T^{LS}_{\ell_b\ell_i,\ell_+\ell_-}|^2. \tag{13}$$

The total cross section is obtained by integrating the differential cross section over E_+ from 0 to E. The proper weight for each matrix element arises from summing over all of the components of L and S [this gives the $(2L+1)(2S+1)$ term] and averaging over the components of ℓ_b and the spin of the core electron and spin of the incoming electron [this gives the $(2\ell_b+1)4$ term]. To show that this is the proper expression for the cross-section differential in E_+, first artificially force the final-state wave function to be zero at a fixed but finite value of r_+ and normalize the $+$ part of the wave function to have a volume integral equal to 1. Thus, there are only quantized energy levels E_+ and inelastic cross sections for having the system in each level in the final state. In the last step, take the limit that this quantization distance goes to infinity to obtain the expression in Eq. (13).

The initial and final states are decomposed into a total angular-momentum representation because the potentials commute with the total angular-momentum operator; this means the total angular momentum and its z component are conserved. Thus, the number of integrals that must be performed can be reduced since the total angular momentum and the z component of the total angular momentum does not depend on whether the wave function is in the 1,2 coordinate system or the $+,-$ system. Furthermore, the T-matrix elements are independent of the z component of the total angular momentum; this means M can be set to zero in the calculation.

Because the total orbital angular-momentum operator is the same in both coordinate systems, the initial and final

states must have the same L and M to give a nonzero matrix element. A very good test of convergence and other problems with the computer programs is to calculate the T-matrix element for final states with an L or M that differs from the initial state. When such a calculation gives results substantially different from zero, then there is a problem with the calculation.

B. Atoms with nonzero angular momentum

The derivation of the T-matrix elements and cross section assumed that the atomic electrons form a closed shell. Actually, very few closed-shell atoms can bind an extra electron (Ca, Sr, and Ba are notable exceptions). In this section, the treatment is generalized to atoms that have nonzero angular momentum. It is shown that when relativistic effects can be ignored, then the atom can be treated as if the atomic electrons have ^1S coupling unless the orientation or alignment of the atom is probed after detachment.

Let L_c, S_c be the orbital angular momentum and spin of the core, $\mathcal{L}_i$, $\mathcal{S}_i$ be the orbital angular momentum and spin of the ion, $\mathcal{L},\mathcal{S}$ be the total orbital angular momentum and spin, and L,S be the orbital angular momentum and spin of the two electrons in the continuum. The T-matrix element for this case can be obtained from Eq. (12) and factors that give the extra angular-momentum coupling of the electrons to the atom. These extra factors arise from projecting the initial-state angular-momentum coupling onto the final-state angular-momentum coupling and are equal to

$$P=\langle (L_c \ell_b)\mathcal{L}_i \ell_i | L_c(\ell_b \ell_i)L\rangle^{\mathcal{L}} \times \langle (S_c s_b)\mathcal{S}_i s_i | S_c(s_b s_i)S\rangle^{\mathcal{S}}, \tag{14}$$

where $s_i=s_b=1/2$ are the spins of the incoming electron and the excess electron, respectively. These terms arise from a recoupling of the angular momenta. The new T-matrix is this factor times the ^1S T-matrix element.

The new T-matrix element can be expressed in terms of six j coefficients and other simple factors:

$$\begin{aligned} T^{\mathcal{L},\mathcal{S}}_{\ell_b \ell_i \mathcal{L}_i \mathcal{S}_i, \ell_+ \ell_- LS} = (-1)^{L_c+\ell_b+\ell_i+\mathcal{L}} [\mathcal{L}_i, L] \begin{Bmatrix} L_c & \ell_b & \mathcal{L}_i \\ \ell_i & \mathcal{L} & L \end{Bmatrix} \\ \times (-1)^{S_c+s_b+s_i+\mathcal{S}} [\mathcal{S}_i, S] \\ \times \begin{Bmatrix} S_c & s_b & \mathcal{S}_i \\ s_i & \mathcal{S} & S \end{Bmatrix} T^{LS}_{\ell_b \ell_i, \ell_+ \ell_-}, \end{aligned} \tag{15}$$

where $T^{LS}_{\ell_b \ell_i, \ell_+ \ell_-}$ is from Eq. (12) and the symbol $[L] = \sqrt{2L+1}$.

The cross-section [20] differential in E_+ is

$$\begin{aligned} \frac{d\sigma}{dE_+} = \frac{2\pi}{E_i} \sum_{\ell_i \ell_+ \ell_- LS\mathcal{L}\mathcal{S}} \frac{(2\mathcal{L}+1)(2\mathcal{S}+1)}{(2\mathcal{L}_i+1)(2\mathcal{S}_i+1)2} \\ \times |T^{\mathcal{L},\mathcal{S}}_{\ell_b \ell_i \mathcal{L}_i \mathcal{S}_i, \ell_+ \ell_- LS}|^2. \end{aligned} \tag{16}$$

The proper weight for each matrix element arises from summing over all of the components of $\mathcal{L}$ and $\mathcal{S}$ [this gives the $(2\mathcal{L}+1)(2\mathcal{S}+1)$ term] and averaging over the components of $\mathcal{L}_i$, $\mathcal{S}_i$ and spin of the incoming electron [this gives the $(2\mathcal{L}_i+1)(2\mathcal{S}_i+1)2$ term]. Using Eq. (6.2.9) of Ref. [21], the identity

$$\sum_{\mathcal{L}} (2\mathcal{L}+1) \begin{Bmatrix} L_c & \ell_b & \mathcal{L}_i \\ \ell_i & \mathcal{L} & L \end{Bmatrix}^2 = \frac{1}{2\ell_b+1} \tag{17}$$

can be shown and a similar one can be shown for the spins. Using Eqs. (15) and (17) in the total cross section [Eq. (16)], the previous expression for the total cross section, Eq. (13), is recovered.

The expression of the energy differential and the total cross section in terms of an expression that completely neglects the angular momenta of the atom will be accurate as long as relativistic effects can be ignored. In practice this means that the orbital for the weakly bound electron does not depend strongly on the spin-orbit interaction; the spin-orbit splitting for the weakly bound electron cannot be a substantial fraction of the binding energy. In practice, this rarely occurs.

C. Monte Carlo integration

The five-dimensional integral for the T-matrix elements are performed numerically with an unweighted Monte Carlo technique using Sobel's sequence of quasirandom numbers [22]. Sobel's sequence of numbers are ''random numbers'' that tend to fill the N-dimensional unit cube more smoothly than pseudorandom number generators, such as the linear congruential generators; the Sobel's sequence of ''random numbers'' converged the integrals with roughly a factor of 2 fewer points. The same sequence of points in the five-dimensional space was used for every T-matrix element so the integration of the differential cross sections could be performed in a reasonable manner.

The radial ranges were chosen so $r_1 \leqslant 6/\sqrt{-2E_b}$ and $r_2 \leqslant 40\pi/\sqrt{2E_i}$. If $s_1(n), s_2(n), s_3(n), s_4(n), s_5(n)$ is the nth five-dimensional point of Sobel's sequence, then the nth point of the spatial integration was

$$\begin{aligned} r_1(n) &= s_1(n) r_{1,\max}, \\ r_2(n) &= s_2(n) r_{2,\max}, \\ \cos\theta_1(n) &= 2s_3(n) - 1, \\ \cos\theta_2(n) &= 2s_4(n) - 1, \\ \phi_2(n) - \phi_1(n) &= 2\pi s_5(n). \end{aligned} \tag{18}$$

The nth point in the $\mathbf{r}_\pm$ coordinates was obtained from the point in $\mathbf{r}_1, \mathbf{r}_2$ coordinates by simple algebra.

Estimates of the convergence with the number of points was obtained by running very large calculations for a few energies and noting the relative errors inherent in the smaller integration. Another technique was to change which component of Sobel's number went with each variable and compare the results from the two different runs. For example, another sequence of random points is generated when $r_1(n) = s_2(n) r_{1,\max}$ and $r_2(n) = s_1(n) r_{2,\max}$, with all other components the same. In general, the integrations are converged to better than 3%.

One difficulty in numerically evaluating the integrals for the T-matrix elements is that a sharp integration boundary in the r_2 coordinate substantially slows the convergence rate with $r_{2,\max}$; this is an inherent property of the integral and does not depend on which numerical method is used. This is a large problem because the number of points needed for the Monte Carlo integration increases roughly linearly with $r_{2,\max}$. The solution was to introduce a ''soft boundary'' in the r_2 direction. This was achieved by replacing the continuum wave in the r_2 direction by a function that was smoothly reduced as the boundary was approached:

$$F_{\ell_i}(r_2) \rightarrow F_{\ell_i}(r_2)\exp[-(2r_2/r_{2,\max})^4]. \tag{19}$$

For small r_2, the exponential hardly changes the continuum function but smoothly cuts off the integration as r_2 approaches the boundary.

The number of integration points is fairly large, usually between 10^5 and 10^6, but not so large that the method could not be implemented on a work station or personal computer. One of the important tricks to speed the evaluation of the integrands involved the four radial functions. For a given $E_i, E_+, \ell_b, \ell_i, \ell_+, \ell_-$, and L, the radial functions were computed on a mesh of equally spaced points. In the Monte Carlo loop over the number of points, the radial functions were interpolated for the value of $r_1(n), r_2(n), \ldots$ using a three-point, quadratic interpolation. Another obvious step was to calculate all Clebsch-Gordon coefficeints outside of the Monte Carlo loop since they do not depend on the value of the five-dimensional point.

D. Large angular momenta

The five-dimensional integrations are very time consuming and thus it makes sense to search for regions where it is not necessary. The most obvious region to investigate is when L becomes large. In this case, the incident electron is always further from the atom than the weakly bound electron. Thus, the incident electron always experiences a repulsive $1/r$ potential, whereas the inner electron only experience the atomic potential. We use these considerations to supplement the calculations of the cross section.

The idea is to use distorted waves in $\mathbf{r}_1, \mathbf{r}_2$ coordinates for the final state for L greater than a maximum value, $L_{\max}$ (i.e., center-of-mass coordinates are used for $L \leqslant L_{\max}$, but single-electron coordinates are used for $L > L_{\max}$). The final states in single-electron coordinates are not as accurate as the center-of-mass coordinates, but it is much more accurate to use this procedure than to use nothing for $L > L_{\max}$; the results converge much faster with $L_{\max}$ when using this top-up procedure.

The only change to the formulation is that instead of the final-state wave function in center-of-mass coordinates the final-state wave function is changed to

$$\psi_j^{(f)} = f_{\ell_1}(r_1) F_{\ell_2}(r_2)[Y_{\ell_1}(\hat{r}_1) Y_{\ell_2}(\hat{r}_2)]_M^L, \tag{20}$$

where $f_{\ell_1}(r)$ is the energy normalized continuum wave calculated in the atomic potential $U(r)$ and $F_{\ell_2}(r)$ is the energy normalized continuum wave calculated in the distorted wave potential $\tilde{U}(r)$ that has the asymptotic form $1/r$.

Because the initial and final states are in the same coordinate system, the T-matrix elements can be evaluated very efficiently. Thus, the T-matrix is calculated from $L_{\max}+1$ to very high L, until the matrix elements become negligibly small. The integrations are performed using a partial-wave expansion of the $1/r_{12}$ potential. The new final-state wave function does not include exchange between the two electrons.

III. THRESHOLD REGION

The behavior of the differential and total cross section in the threshold region was originally discussed in Ref. [16]. In this region, $E \simeq 0$, which means $E_i \simeq -E_b$ and $E_+ \simeq 0$ and $E_- \simeq 0$. Their results may be rederived in a brief manner by investigating the behavior of the continuum functions in the expression for the T-matrix element, Eq (12). In Ref. [16], it was shown that the main contribution to the T-matrix element was from the region of space near the atom. The incident continuum wave hardly changes with energy in the threshold region since the incident energy hardly changes in this region; thus, this function contributes no energy dependence in the threshold region. Because the momentum in the $+$ coordinate is small, the Bessel function hardly changes over the reaction region; thus, contribution to the T-matrix elements from the continuum motion of the center of mass is proportional to $\sqrt{k_+} \propto E_+^{1/4}$. The continuum wave in the $-$ coordinate contributes a very rapidly varying function with E_- since small r_- is in the tunneling region; the tunneling factor can be obtained from a WKB(J) approximation using

$$\sqrt{2}\int_0^{1/\sqrt{2}E_-}\left(\frac{1}{\sqrt{2}r_-} - E_-\right)^{1/2} dr_- = \frac{\pi}{2\sqrt{E_-}} \tag{21}$$

to obtain a factor for the T-matrix that is proportional to $\exp(-\pi/2\sqrt{E_-})$; the tunneling factor is calculated as if the electron needs to tunnel from the origin to the classically allowed region.

The threshold behavior of the cross section may be obtained by squaring these contributions to the T-matrix elements and by noting that E_i is nearly constant near threshold. This gives

$$\frac{d\sigma}{dE_+} = C\sqrt{E_+}\exp(-\pi/\sqrt{E-E_+}), \tag{22}$$

where C is an E-independent constant and all energies are in atomic units. The integration over E_+ may be performed to give the threshold dependence of the total cross section. The change of variables $E_+ = E\sin^2\beta$ and $dE_+ = 2E\sin\beta\cos\beta d\beta$ give

$$\begin{aligned}\sigma(E) &= 2CE^{3/2}\int_0^{\pi/2}\sin^2\beta\cos\beta\exp\left(-\frac{\pi}{\sqrt{E}\cos\beta}\right)d\beta \\ &\simeq 2CE^{3/2}\exp\left(-\frac{\pi}{\sqrt{E}}\right)\int_0^{\infty}\beta^2\exp\left(-\frac{\pi\beta^2}{2\sqrt{E}}\right)d\beta \\ &= C\sqrt{\frac{2}{\pi}}E^{9/4}\exp\left(-\frac{\pi}{\sqrt{E}}\right),\end{aligned} \tag{23}$$

where all energies are in atomic units. This function decreases extremely rapidly as $E \to 0$.

The main difficulty with threshold laws is in knowing the range of validity. In Ref. [16], it was estimated that $E \ll 0.4$ eV for electron-impact detachment of H^-. Unfortunately, the cross section decreases very rapidly for energies less than 0.4 eV. At $E = 0.37$ eV the total cross section is $\simeq 1/40$ Mb, whereas it is $\simeq 1/2$ b ($1\text{b} = 10^{-24}$ cm^2) at $E = 0.19$ eV. Thus, there is no hope for an experimental test of this law. It is also extremely difficult to test this law using Eq. (12) because the convergence of the integrals becomes extremely slow for $E < 0.3$ eV.

The threshold law for electron-impact detachment can be extended by a more careful analysis of the behavior of the functions in Eq. (12). This will allow the application of the threshold law over a larger range of energies so it can be tested experimentally and theoretically. The first important point to note is that the substantial part of the integral is from the region of space where $r_2 \sim 1/E_i$ and $r_1 \sim 1/\sqrt{-2E_b}$. Also, the electrostatic repulsion causes $r_- \simeq (r_2 + r_1)/\sqrt{2}$ and $r_+ \simeq (r_2 - r_1)/\sqrt{2}$.

The difficulty in finding the behavior of the *T*-matrix element is in knowing what region of space gives the main contribution in the integrals; it may be surprising that the main contribution to the integral is in the region of space near the turning point of the incoming wave and *not* in the region near the turning point for the final state. Clearly, the region with $r_2 < 1/E_i$ is not important because this region is not classically allowed for the incident electron. For the region $r_2 \sim 1/E_i$, the continuum wave for the incident electron oscillates with increasing r_2. In the classically allowed region, this continuum wave can be usefully expressed as the imaginary part of an outgoing wave. Because the functions in the integral for the *T*-matrix are analytic, the integration path can be deformed to go into the complex plane for r_2; instead of integrating along the real r_2 line, the contour of integration is deformed to go into the complex plane to $i\infty$; the continuum wave then becomes a rapidly decreasing exponential function. Thus, most of the integral is accumulated near the turning point, $r_2 \sim 1/E_i$.

There are several changes to the integrand that arise from having the main region be near $r_2 \sim 1/E_i$ instead of $r_2 \sim 0$. Because $r_1 \ll r_2$, the value of $r_\pm \sim r_2/\sqrt{2}$. The largest change to the threshold law is that the tunneling factor changes to

$$\Phi_{\mathrm{WKB(J)}}(E_-, E_i) = \sqrt{2} \int_{1/\sqrt{2}E_i}^{1/\sqrt{2}E_-} \left(\frac{1}{\sqrt{2}r_-} - E_- \right)^{1/2} dr_- = \frac{\pi}{2\sqrt{E_-}} \left\{ 1 - \frac{2}{\pi} [\arcsin(x) + x\sqrt{1-x^2}] \right\}, \tag{24}$$

where $x = \sqrt{E_-/E_i}$. This shows that the correction to the exponential in the threshold goes to zero as threshold is approached because $x \to 0$ as threshold is approached. However, the correction goes to zero very slowly since it goes as the square root of the excess energy does.

There are a few other corrections that have a smaller effect. The contribution from the continuum wave of the center of mass remains the same since the Bessel function is slowly varying. The only other terms are those proportional to E_i. There are four terms that contribute factors of E_i to the *T*-matrix element. The potential terms give a contribution of $1/r_2^2$, which is proportional to E_i^2. There is a term proportional to $E_i^{-1/4}$ from the incident continuum wave. From the amplitude of the r_- continuum function, there is a term proportional to $r_-^{1/4}$, which is proportional to $E_i^{-1/4}$. And, from the integration into the complex plane is a factor of $E_i^{-1/2}$. Thus,

$$T \propto E_i \sqrt{k_+} \exp[-\Phi_{\mathrm{WKB(J)}}(E_-, E_i)] \tag{25}$$

in the region near threshold. Substituting this form into the cross section gives

$$\frac{d\sigma}{dE_+} = C E_i \sqrt{E_+} \exp[-2\Phi_{\mathrm{WKB(J)}}(E - E_+, E_i)] \tag{26}$$

for the threshold law. This differs from the original threshold law by the factor of E_i and by the WKB(J) tunneling integral not going all of the way to the origin.

The threshold law for the total cross section may be obtained by performing the same change of variables as above: $E_+ = E\sin^2\beta$ and $dE_+ = 2E\sin\beta\cos\beta$. This gives a total cross section with the form

$$\sigma(E) \propto E_i E^{9/4} G(\sqrt{E/E_i}) \exp[-2\Phi_{\mathrm{WKB(J)}}(E, E_i)], \tag{27}$$

where $G(x) = 1 - 2[\arcsin(x) - x\sqrt{1-x^2}]/\pi$ arises from the derivative of the WKB(J) phase with respect to E_-. In the limit $E \to 0$, this form for the threshold cross section is identical to Eq. (23). It is interesting to note that some of the generic properties of this threshold law are also observed in Refs. [23] and [24], where there is a Coulomb interaction with the heavy particle. These properties include the reaction zone being defined in the incoming channel, an energy dependence for the size of the reaction zone, and the main energy dependence arising from a WKB(J) tunneling factor.

Recently, the threshold law for electron-impact detachment was reexamined from a classical formulation. This threshold law, from Ref. [15], appears to be quite different from the law in Eq. (27). However, the basic idea about which processes control the threshold behavior is the same. The idea is that the electrons must tunnel out from the region where the incident electron reaches its turning point. Thus, the main energy dependence, which comes from the WKB(J) integral, is exactly the same. The only difference is in the energy dependence of the prefactor. Using the notation of this paper the threshold law from Ref. [15] is

$$\sigma(E) \propto (\tilde{b}_0 + E_i)^{-1} \exp[-2\Phi_{\mathrm{WKB(J)}}(E, E_i)], \tag{28}$$

where $\tilde{b}_0 = (b_0 - 1)|E_b|$ with the $b_0 = 119$ from Ref. [15]. The reason for the difference of the prefactors is that Ref. [15] did not account for energy going into the center-of-mass motion and only used the differential cross section at the point $E_+ = 0$ or, equivalently, $E_- = E$. However, the cross section is exactly 0 for this energy because of the Wigner threshold law $E_+^{1/2}$ in the center-of-mass motion.

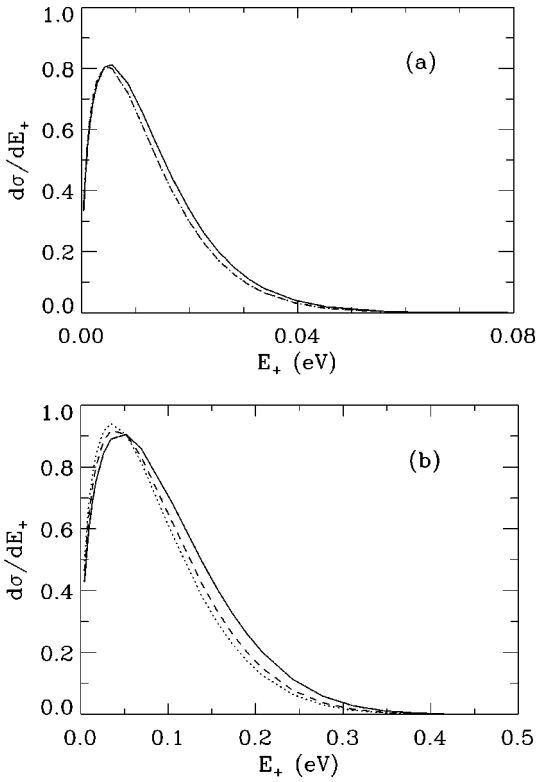

FIG. 1. Differential cross section in arbitrary units from the full calculation (solid line) and from the threshold laws from Eq. (22) (dotted line) and Eq. (26) (dashed line). (a) At $E=0.19$ eV, total energy; the two threshold laws give nearly identical results at this energy. (b) At $E=0.75$ eV, total energy.

In Fig. 1, the differential cross section for detachment from H^- is plotted for the full numerical calculation and the different forms of the threshold law, Eqs. (22) and (26). The two energies are for $E_i \sim 25\%$ higher than threshold ($E/E_i \sim 1/4$) and for E_i roughly twice threshold. The interesting feature is that the two forms of the threshold law give very similar shapes so they agree roughly equally well with the shape of the full calculation [25]. They both agree fairly well with the differential cross section considering the large change in the total cross section. However, there is an enormous difference between the two forms in that the coefficeint used to match the height of the differential cross section is changed by a factor of ~ 150 for the simple threshold law and a factor of ~ 0.6 for the extended threshold law.

In Fig. 2, the total cross section for detachment from H^- is plotted for the full numerical calculation and the different forms of the threshold law, Eqs. (23), (27), and (28). All of the threshold laws are scaled to give the total cross section at the lowest energy point. Although the total cross section changes by over 7 orders of magnitude in this energy range, the extended threshold law, Eq. (27), agrees with the full calculation to within 40%, while the simple threshold law, Eq. (23), differs by up to a factor of ~ 150. The reason for the relative size of the errors is that in the simple threshold law, the electrons must tunnel too far in the final state; they do not need to tunnel out from $r_- \sim 0$, only from $r_- \sim 1/\sqrt{2}E_-$. This causes the cross section to decrease too fast as $E \to 0$. The threshold law [15] given in Eq. (28) is too small by a factor of ~ 30 at the highest energy point. However, it is important to stress that all of the threshold laws discussed here agree with each other in the sense that they have the same dominant functional form as $E \to 0$.

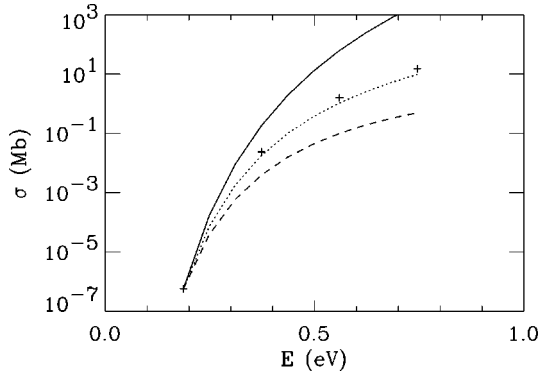

FIG. 2. Total detachment cross section for H^- using the full calculation (crosses) and the threshold laws from Eq. (23) (solid line), from Eq. (27) (dotted line), and from Eq. (28) (dashed line).

These figures suggest that the extended threshold law gives a reasonable description of the electron-impact detachment process. However, it must be remembered that the theoretical method used to *test* the threshold law was also used to *derive* it. The agreement in Figs. 1 and 2 only shows that the analysis of the behavior of the functions in Eq. (12) was substantially correct. I expect that the relative size of the *T*-matrix elements from Eq. (12) is more accurate in the threshold region than in any other energy range, but this has not been shown. A serious test of the threshold law requires a completely different style of calculation or requires an experiment. The analysis of the threshold behavior from Ref. [15] does provide a completely different treatment but gives a law that is somewhat different from that derived here.

Unfortunately, it will be difficult to experimentally test the threshold law for electron-impact detachment. The problem is that the cross section is small over the range where the threshold law may be expected to hold and it decreases extremely rapidly as $E \to 0$. It seems likely that the threshold law will hold for $E < -E_b$ and it may extend to energies somewhat higher. In an experimental test of the threshold law, there will be two competing effects that determine the choice of atom to use as a test case. The maximum of the total cross section increases as the binding energy is reduced; thus, using an atom with a smaller binding energy will increase the signal. However, the energy scale becomes compressed as the binding energy is reduced; thus, using an atom with a larger binding energy will decrease the need for high-energy resolution for the incident electrons. As an example from H^-, I have compared the relative change in the cross section from an incident energy of 1.31–1.50 eV. The large *T*-matrix calculation gives an increase in cross section of a factor of 9.6, whereas the threshold law from Ref. [16] gives a factor of 36, from Ref. [15] gives a factor of 5.0, and from Eq. (27) gives a factor of 9.1. In principle, these differences are measurable so it may be possible to test which threshold law best describes electron detachment in H^- although the cross section is small (1.6 Mb at 1.31 eV and 15.3 Mb at 1.50 eV).

IV. RECOIL OF THE ATOM

The differential cross section in Fig. 1 holds an interesting implication for the recoil of the atom after the excess elec-

tron is detached. In our treatment, the atom is infinitely heavy but, in actuality, it is only 10^4-10^6 times heavier than the electron. Because the atom interacts with the two electrons, the total momentum of the two electrons is not conserved and the atom can gain momentum during the detachment process. The momentum given to the atom is the initial momentum of the two electrons minus the final momentum of the two electrons.

The initial momentum of the two electrons arises solely from the incident electron. In atomic units, the initial total momentum is $\sqrt{2E_i}$. The final momentum is $\sqrt{2}\mathbf{p}_+$, where $\mathbf{p}_+$ is the momentum in the + coordinate and has a magnitude $\sqrt{2E_+}$. In the threshold region, $E \ll E_i$ and from Fig. 1 most of the scattering probability is for $E_+ \sim 0.1E$. Thus, the final momentum is very small compared to the initial momentum.

The implication is that the momentum given to the atom in the threshold region is nearly equal to the momentum of the incident electron. At much higher energies, the incident electron is hardly deflected and only a small fraction of the incident momentum is given to the atom. This apparently paradoxical behavior can be understood by noting that the detachment in the threshold region occurs when the incident electron is at the closest distance $r \sim 1/E_i$. At this point, the incident electron has lost all of its initial momentum and the negative ion has gained all of the initial momentum. Once the electron is detached from the atom, the two electrons cannot change their total momentum (an external potential is needed) which is nearly 0. Thus, the atom retains the momentum given to the negative ion. At high energies, the reverse situation holds in that the detachment occurs from weak interaction between the incident electron and the negative ion when the electron is far from the ion; thus the incident electron's momentum remains nearly unchanged and the atom only acquires a small fraction of the incident momentum.

V. SCALING THE CROSS SECTION

In Ref. [14], a method for scaling the cross section was proposed which only used the asymptotic form of the wave function and the binding energy. This scaling rule for the cross section is not expected to be exact but can serve as a guide for making quick estimates using data from another atom.

The idea is to use the properties of the functions in the T-matrix elements. One important feature that is used is the weak dependence of the T-matrix elements on the precise form of the potential for the incoming electron, $\tilde{U}(r)$. In all of the calculations, a screened, repulsive Coulomb potential was used but the cross section changed by less than 10–20 % when using $\tilde{U}(r)=1/r$ for all distances. This form will be used in the discussion below.

The main point to note is that the energy scale is set by the binding energy, $-E_b$, and the distance scale is set by the size of the negative ion, $\sim 1/\kappa_b = 1/\sqrt{-2E_b}$. Thus, all functions will be written in terms of scaled distances, $r = r_{\rm scal}/\kappa_b$, where r is meant to indicate any of the distances, and scaled energies, $\epsilon = \epsilon_{\rm scal}\kappa_b^2$, where ϵ is meant to indicate any of the energies. All of the continuum functions have the form

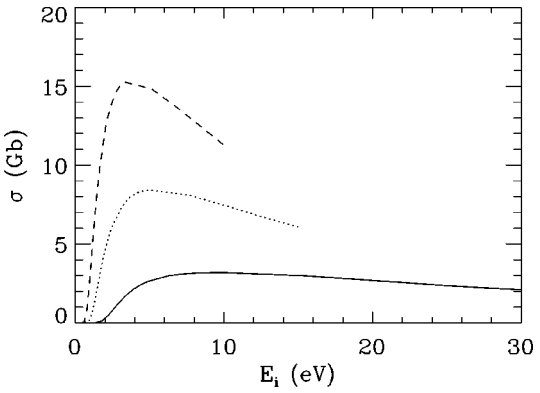

FIG. 3. Total cross section for H^- (solid line, $N_b=1.51$), H^--like ion with 1/2 the binding energy (dotted line, $N_b=1.33$), and H^--like ion with 1/3 the binding energy (dashed line, $N_b=1.26$).

$$f \propto \frac{1}{r\sqrt{k}}\bar{f}(kr), \tag{29}$$

where $k=\sqrt{2\epsilon}$ and the $\bar{f}$ does not have a strong energy dependence. The bound function has the form

$$R \propto \frac{N_b\sqrt{\kappa_b}}{r}\exp(-\kappa_b r), \tag{30}$$

where N_b is the asymptotic normalization.

Now the form of the cross section can be approximated by examining the scaling of all the functions in the T-matrix, Eq. (12). From the four orbitals, there is a $1/r^4$ which gives κ_b^4. From the potentials, there is $1/r$ which gives κ_b. From the volume element $(dV_1 dV_2)$, there is a r^6 which gives $1/\kappa_b^6$. From the energy dependent amplitude of the four orbitals there is a factor of N_b/κ_b. Multiplying all of these factors gives a T-matrix proportional to N_b/κ_b^2.

To make the total cross section, the T-matrix is squared and divided by the incident energy and integrated over the allowed range of E_+. These last two energy terms cancel to give

$$\sigma(E) = \frac{N_b^2}{E_b^2}\sigma_{\rm scal}(E/|E_b|), \tag{31}$$

where $\sigma_{\rm scal}$ is a scaled cross section that does not depend on the binding energy. The normalization constant N_b should not vary much with binding energy as the binding energy goes to 0. However, for the binding energies in the range of $0.5-1.0$ eV, it may give effects at the 20–40 % level.

In Fig. 3, calculations for model atoms are given that show the level of variation in the cross section that may be expected when changing the binding energy. One calculation is for detachment from H^-, while the other two are for a H^--like ion (s-wave attached electron) but with binding energies a factor of 2 and 3 less than for H^-. In Fig. 4, the cross sections are scaled so that the energies are given in units of the binding energy and the cross section is multiplied by E_b^2/N_b^2. Now the cross sections appear very similar.

There are a few considerations that reduce the accuracy of the scaling rule. The first is that the final state is not exact

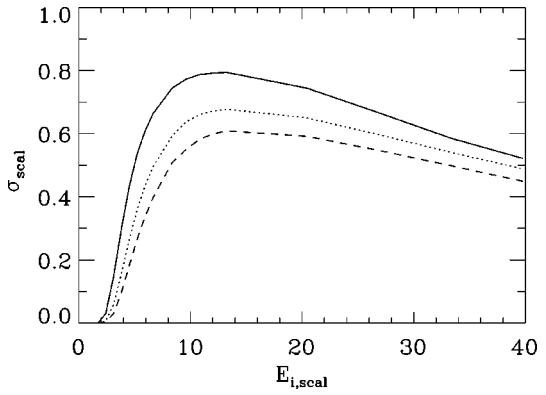

FIG. 4. Same as Fig. 3 but the incident energy is scaled by the binding energy and the cross section is scaled as in Eq. (32). The units of the scaled cross section are Gb eV^2 and $E_{i,scal}$ is dimensionless.

and taking the potential for the incident electron to be $1/r$ for all distances introduces some error. The main source of error is that the continuum waves for the repulsive Coulomb interaction cannot be written in the form of Eq. (29); the turning point for a repulsive Coulomb potential is at distances proportional to $1/\epsilon$ and not $1/\sqrt{\epsilon}$. There are energy dependent phases that can be important. The reason that the scaling rule works as well as it does is because the main contribution to the integral comes from phase-matching conditions for the continuum waves in the classically allowed region of space. In this region, phase is proportional to $\sqrt{\epsilon}r$ plus more slowly varying terms that are not very important.

VI. CONCLUSIONS

In this paper, the details of recent calculations of electron-impact detachment of negative ions have been presented. The calculations are based on the idea that correlation is small in both the initial state (an incoming electron and an electron attached to an atom) and the final state (two freely moving electrons and an atom) *if* the proper coordinate system is used to describe each. For the initial state, the proper coordinate system is that of the individual electrons, $\mathbf{r}_1, \mathbf{r}_2$. For the final state, the proper coordinate system is the center-of-mass coordinates for the electron, $\mathbf{r}_{\pm} = (\mathbf{r}_2 \pm \mathbf{r}_1)/\sqrt{2}$.

The resulting formalism was used to investigate the behavior of the total cross section near threshold. This has led to an extension of the threshold law to a form that might be experimentally testable. The main correction to the threshold law from Ref. [16] arises from not forcing the electron to tunnel from the origin into the classically allowed region; the main correction to the threshold law from Ref. [15] arises from allowing energy to also be distributed into the center-of-mass motion. An analysis of the detachment cross-section differential in energy shows that in the low-energy region the atom recoils with a momentum nearly equal to the momentum of the incident electron; this is an apparently paradoxical behavior since the recoil momentum becomes a *larger* fraction of the incident momentum as the energy of the incident electron decreases to the threshold energy. Finally, the behavior of the cross section as the binding energy changes (with all other properties remaining fixed) roughly agrees with the scaling law proposed in Ref. [14]; thus, the energies scale with the binding energy of the negative ion and the cross section scales inversely with square of the binding energy.

ACKNOWLEDGMENTS

I acknowledge discussions of several aspects of this problem with M.S. Pindzola and discussions of the threshold law with P.F. O'Mahony. I thank J.M. Rost for sending parameters for the threshold law and for pointing out the important features of Ref. [15]. This work was supported by the U.S. DOE. Computations were performed at the National Energy Research Supercomputer Center in Berkeley, CA. This work is part of the research program of the ''Stichting voor Fundamenteel Onderzoek der Materie (FOM),'' which is financially supported by the ''Nederlandse organisatie voor Wetenschappelijke Onderzoek (NWO).''

[1] G. Tisone and L. M. Branscomb, Phys. Rev. Lett. **17**, 236 (1966); Phys. Rev. **170**, 169 (1968).
[2] D. F. Dance, M. F. A. Harrison, and R. D. Rundel, Proc. R. Soc. London, Ser. A **299**, 525 (1967).
[3] B. Peart, D. S. Walton, and K. T. Dolder, J. Phys. B **3**, 1346 (1970).
[4] B. Peart, R. Forrest, and K. T. Dolder, J. Phys. B **12**, L115 (1979); **12**, 847 (1979).
[5] L. H. Andersen, D. Mathur, H. T. Schmidt, and L. Vejby-Christensen, Phys. Rev. Lett. **74**, 892 (1995).
[6] L. Vejby-Christensen *et al.*, Phys. Rev. A **53**, 2371 (1996).
[7] T. Tanabe *et al.*, Phys. Rev. A **54**, 4069 (1996).
[8] L. H. Andersen *et al.*, Phys. Rev. A **58**, 2819 (1998).
[9] F. Robicheaux, R. P. Wood, and C. H. Greene, Phys. Rev. A **49**, 1866 (1994).
[10] M. S. Pindzola, Phys. Rev. A **54**, 3671 (1996).
[11] V. N. Ostrovsky and K. Taulbjerg, J. Phys. B **29**, 2573 (1996).
[12] A. K. Kazansky and K. Taulbjerg, J. Phys. B **29**, 4465 (1996).
[13] J. T. Lin, T. F. Jiang, and C. D. Lin, J. Phys. B **29**, 6175 (1996).
[14] F. Robicheaux, Phys. Rev. Lett. **82**, 707 (1999).
[15] J. M. Rost, Phys. Rev. Lett. **82**, 1652 (1999).
[16] R. W. Hart, E. P. Gray, and W. P. Guier, Phys. Rev. **108**, 1512 (1957).
[17] T. Ohmura and H. Ohmura, Phys. Rev. **118**, 154 (1960).
[18] C. L. Pekeris, Phys. Rev. **126**, 1470 (1962).
[19] C. Froese Fischer, A. Ynnerman, and G. Gaigalas, Phys. Rev. A **51**, 4611 (1995).
[20] R. K. Nesbet, *Variational Methods in Electron-Atom Scattering Theory* (Plenum Press, New York, 1980), Chap. 1.2.
[21] A. R. Edmonds, *Angular Momentum in Quantum Mechanics* (Princeton University Press, Princeton, N.J., 1974).

[22] W. H. Press, S. A. Teukolsky, W. T. Vetterling, and B. P. Flannery, *Numerical Recipes*, 2nd ed. (Cambridge University Press, Cambridge, New York, 1992).

[23] W. Ihra, F. Mota-Furtado, and P. F. O'Mahony, Phys. Rev. A **55**, 4263 (1997).

[24] P. Chocian, W. Ihra, and P. F. O'Mahony, Phys. Rev. A **57**, 3583 (1998).

[25] The $L=0$ contribution to the differential cross section was very small in the full calculation. Roughly half of the contribution to the cross section was from the $L=1$ incident wave.